Total Structure Determination of Apratoxin A, a Potent Novel Cytotoxin from the Marine Cyanobacterium *Lyngbya majuscula*

Hendrik Luesch,[†] Wesley Y. Yoshida,[†] Richard E. Moore,*[,†] Valerie J. Paul,*[,‡] and Thomas H. Corbett[§]

Contribution from the Department of Chemistry, University of Hawaii at Manoa, Honolulu, Hawaii 96822, University of Guam Marine Laboratory, UOG Station, Mangilao, Guam 96923, and Karmanos Cancer Center, Wayne State University, Detroit, Michigan 48201

Received February 20, 2001

Abstract: Apratoxin A (**1**), a potent cytotoxin with a novel skeleton, has been isolated from the marine cyanobacterium *Lyngbya majuscula* Harvey ex Gomont. This cyclodepsipeptide of mixed peptide−polyketide biogenesis bears a thiazoline ring flanked by polyketide portions, one of which possesses an unusual methylation pattern. Its gross structure has been elucidated by spectral analysis, including various 2D NMR techniques. The absolute configurations of the amino acid-derived units were determined by chiral HPLC analysis of hydrolysis products. The relative stereochemistry of the new dihydroxylated fatty acid unit, 3,7-dihydroxy-2,5,8,8-tetramethylnonanoic acid, was elucidated by successful application of the *J*-based configuration analysis originally developed for acyclic organic compounds using carbon−proton spin-coupling constants ($^{2,3}J_{C,H}$) and proton−proton spin-coupling constants ($^{3}J_{H,H}$); its absolute stereochemistry was established by Mosher analysis. The conformation of **1** in solution was mimicked by molecular modeling, employing a combination of distance geometry and restrained molecular dynamics. Apratoxin A (**1**) possesses IC_{50} values for in vitro cytotoxicity against human tumor cell lines ranging from 0.36 to 0.52 nM; however, it was only marginally active in vivo against a colon tumor and ineffective against a mammary tumor.

Introduction

Cyanobacteria produce an elaborate array of secondary metabolites exhibiting a broad spectrum of bioactivities.[1] While some toxic metabolites pose a health threat,[2] cyanobacteria are a recognized source of potential pharmaceuticals.[3] For example, cryptophycin-52, a synthetic analogue of the terrestrial cyanobacterial peptolide cryptophycin-1,[4] recently entered phase II human clinical trials against cancer. Dolastatin 10,[5] a modified pentapeptide isolated originally from the sea hare *Dolabella auricularia* and more recently from a marine cyanobacterium,[6] is another antitumor agent being clinically evaluated.[7]

In our ongoing efforts toward finding novel marine cyanobacterial metabolites with antitumor activity, we have been investigating a variety of the cyanobacterium *Lyngbya majuscula* Harvey ex Gomont from Finger's Reef, Apra Harbor, Guam, which closely resembles a more recently defined taxonomic species, *L. bouillonii* Hoffmann et Demoulin.[8] This organism, collected over a period of several years, has proven to be exceptionally rich in secondary metabolites. We have already reported the discovery of the cytotoxic peptolides lyngbyastatin 2,[9] norlyngbyastatin 2,[9] and lyngbyabellins A[10] and B,[11] all of which are analogues of compounds previously isolated from *D. auricularia*. In addition, the isolation of noncytotoxic lipopeptides apramides A−G from extracts of this cyanobacterium has been described.[12] Herein we report the isolation, total structure elucidation, and antitumor evaluation of apratoxin A (**1**), the most potent cytotoxin produced by this organism.

Results and Discussion

Isolation. Cyanobacterial collections from Finger's Reef, Apra Harbor, Guam, were freeze-dried and extracted with various organic solvents. Cytotoxicity-guided solvent partition

* To whom correspondence should be addressed. R.E.M.: Phone: (808) 956-7232. Fax: (808) 956-5908. E-mail: moore@gold.chem.hawaii.edu. V.J.P.: Phone: (671) 735-2186. Fax: (671) 734-6767. E-mail: vpaul@uog9.uog.edu.

[†] University of Hawaii at Manoa.

[‡] University of Guam Marine Laboratory.

[§] Wayne State University.

(1) Moore, R. E. *J. Ind. Microbiol.* **1996**, *16*, 134−143.

(2) (a) Yasumoto, T.; Murata, M. *Chem. Rev.* **1993**, *93*, 1897−1909. (b) Moore, R. E.; Ohtani, I.; Moore, B. S.; de Koning, C. B.; Yoshida, W. Y.; Runnegar, M. T. C.; Carmichael, W. W. *Gazz. Chim. Ital.* **1993**, *123*, 329−336.

(3) Jaspars, M.; Lawton, L. A. *Curr. Opin. Drug Discovery Dev.* **1998**, *1*, 77−84.

(4) (a) Trimurtulu, G.; Ohtani, I.; Patterson, G. M. L.; Moore, R. E.; Corbett, T. H.; Valeriote, F. A.; Demchik, L. *J. Am. Chem. Soc.* **1994**, *116*, 4729−4737. (b) Barrow, R. A.; Hemscheidt, T.; Liang, J.; Paik, S.; Moore, R. E.; Tius, M. A. *J. Am. Chem. Soc.* **1995**, *117*, 2479−2490. (c) Golakoti, T.; Ogino, J.; Heltzel, C. E.; Husebo, T. L.; Jensen, C. M.; Larsen, L. K.; Patterson, G. M. L.; Moore, R. E.; Mooberry, S. L.; Corbett, T. H.; Valeriote, F. A. *J. Am. Chem. Soc.* **1995**, *117*, 12030−12049.

(5) Pettit, G. R.; Kamano, Y.; Herald, C. L.; Tuinman, A. A.; Boettner, F. E.; Kizu, H.; Schmidt, J. M.; Baczynskyj, L.; Tomer, K. B.; Bontems, R. *J. Am. Chem. Soc.* **1987**, *109*, 6883−6885.

(6) We recently isolated dolastatin 10 from a marine cyanobacterium: Luesch, H.; Moore, R. E.; Paul, V. J.; Mooberry, S. L.; Corbett, T. H. *J. Nat. Prod.* Submitted for publication.

(7) Some other lead compounds that have been isolated from marine invertebrates are suspected to be biosynthesized by symbiotic microorganisms such as cyanobacteria: (a) Moore, R. E.; Banarjee, S.; Bornemann, V.; Caplan, F. R.; Chen, J. L.; Corley, D. G.; Larsen, L. K.; Moore, B. S.; Patterson, G. M. L.; Paul, V. J.; Stewart, J. B.; Williams, D. E. *Pure Appl. Chem.* **1989**, *61*, 521−524. (b) Faulkner, D. J.; Harper, M. K.; Haygood, M. G.; Salomon, C. E.; Schmidt, E. W. In *Drugs from the Sea*; Fusetani, N., Ed.; Karger: Basel, 2000; pp 107−119.

(8) Hoffmann, L.; Demoulin, V. *Belg. J. Bot.* **1991**, *124*, 82−88.

(9) Luesch, H.; Yoshida, W. Y.; Moore, R. E.; Paul, V. J. *J. Nat. Prod.* **1999**, *62*, 1702−1706.

(10) Luesch, H.; Yoshida, W. Y.; Moore, R. E.; Paul, V. J.; Mooberry, S. L. *J. Nat. Prod.* **2000**, *63*, 611−615.

10.1021/ja010453j CCC: $20.00
Published on Web 05/15/2001

followed by normal-phase chromatography and reversed-phase HPLC afforded apratoxin A (**1**) as a colorless, amorphous solid {$[\alpha]^{25}_D$ −161 (*c* 1.33, MeOH)}.

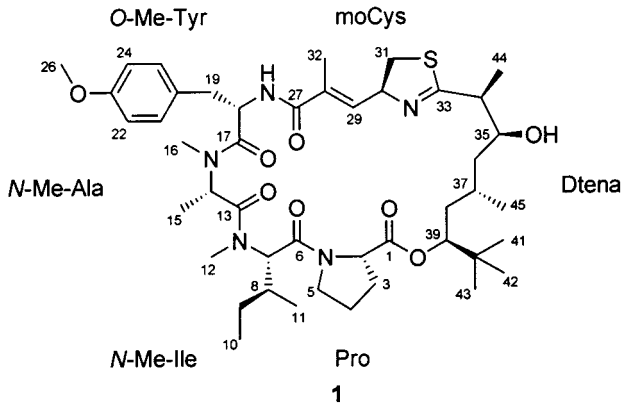

1

Gross Structure. NMR data coupled with a $[M + H]^+$ peak at *m*/*z* 840.4974 in the HRFABMS of **1** suggested a molecular formula of $C_{45}H_{69}N_5O_8S$ (calcd for $C_{45}H_{70}N_5O_8S$, 840.4945). Further NMR analysis (^{1}H, ^{13}C, HSQC, ^{1}H−^{1}H COSY, and HMBC, see Table 1) in $CDCl_3$ revealed the presence of three methylated amino acid moieties (*O*-methyltyrosine, *N*-methylalanine, *N*-methylisoleucine), one regular amino acid unit (proline), and an α,*β*-unsaturated modified cysteine residue (moCys, C27−C32) containing a trisubstituted double bond. The geometry of the double bond was concluded to be *E* since a ROESY experiment showed a cross-peak between the methyl signal at *δ* 1.96 (H_3-32) and the methine signal at *δ* 5.25 (H-30). The chemical shifts for H-30 (*δ* 5.25) and H_2-31ab (*δ* 3.14 and 3.46) as well as the HMBC correlations of these protons to a carbon at *δ* 177.4 (C33) strongly suggested that these nuclei were present in a thiazoline ring. The last residue was classified as a polyketide-derived unit possessing a high degree of methylation (C33−C45). Most prominent in the ^{1}H NMR spectrum was an intense singlet at *δ* 0.87 attributed to a *tert*-butyl group, a unique feature of this residue. Oxygenation of C35 and C39 was revealed from ^{13}C NMR data (δ_{C35} 71.6, δ_{C39} 77.4). The methine proton H-35 (*δ* 3.54) was coupled to an exchangeable proton (δ_{OH} 4.69) indicating that an OH was attached to C35, whereas the chemical shift for H-39 (*δ* 4.97) indicated that an acyloxy group was on C39. The presence of hydroxyl and ester functionalities were consistent with IR absorptions at 3412 (broad) and 1733 cm^{-1}, respectively, the most predominant IR bands in addition to the broad amide band with its absorption maximum at 1623 cm^{-1}. ^{1}H−^{1}H COSY and HMBC analysis (Table 1) revealed the location of additional methyl groups at C34 and C37, and ultimately disclosed the last partial structure as the new dihydroxylated fatty acid moiety, 3,7-dihydroxy-2,5,8,8-tetramethylnonanoic acid (Dtena). The linear sequence (*N*-Me-Ile)-(*N*-Me-Ala)-(*O*-Me-Tyr)-moCys-Dtena-Pro was established from HMBC data and confirmed by a ROESY experiment (Table 1). A strong cross-peak in the ROESY spectrum between the signal at *δ* 4.23 of Pro (H-5b) and the doublet at *δ* 5.20 of the *N*-Me-Ile residue (H-7) suggested the connection of these two amino acid units, leading to the macrocyclic gross structure depicted in structure **1**.

Stereochemistry. Acid hydrolysis of **1** followed by chiral HPLC analysis of the amino acid hydrolyzate revealed L configuration for the Pro, *N*-Me-Ile, *N*-Me-Ala, and *O*-Me-Tyr (all *S*). Ozonolysis and oxidative workup prior to acid hydrolysis led to cysteic acid which was determined to be the D-isomer by chiral HPLC; this meant that the stereochemistry at C30 in **1** was *S*.

J-based configuration analysis,[13] a recently developed powerful method for the elucidation of relative stereochemistry in acyclic structures using $^3J_{H,H}$ and $^{2,3}J_{C,H}$ values,[14] was successfully applied to the polyketide portion C33−C45 (Dtena unit) in **1** to solve the configurations of the last four stereocenters. Its application to cyclic systems has only little precedence[15] and this may be due to the concern of nonstaggered conformations being present.[13] In large macrocyclic compounds such as **1**, however, only staggered conformations should exist. $^3J_{H,H}$ values were measured by 1D TOCSY[16] and homonuclear decoupling experiments, and $^{2,3}J_{C,H}$ values by sensitivity- and gradient-enhanced hetero (ω_1) half-filtered TOCSY (HETLOC)[17] or 2D gradient-selected HSQMBC.[18] Diagonal peaks obscured some of the important cross-peaks in the HETLOC spectrum. In those instances coupling constants were obtained by employing a modified pulse sequence (Figure 1), where a diagonal inversion component[19] was appended to the original pulse sequence[17] to provide nondiagonal spectra.[20] The HSQMBC experiment was used for measuring coupling constants of protons to the nonprotonated carbons C33 and C40, and when the magnetization transfer by TOCSY was small.[18,21] All observed homonuclear and heteronuclear coupling constants were either small or large and therefore fit the model. No intermediate value was measured and this indicated the presence of one dominant conformer possessing no significant deviation from anti or gauche orientations (<10°) along the chain.[13,22]

For the relative stereochemistry of the 1,2-methine system along C34−C35, $^{2,3}J_{C,H}$ values could not be used to distinguish between the two possible rotamers (*threo* A-3, *erythro* B-3)[23] with H-34/H-35 anti configuration ($^3J_{H\text{-}34,H\text{-}35}$ = 10.0 Hz).[13] However, NOE experiments revealed spatial proximity for H-34 and (lowfield) H-36b and for H_3-44 and (highfield) H-36a,[24] but none for H_3-44 and the OH proton;[25] taken together, this was only in agreement with the *erythro* rotamer B-3 (Figure 2a). All other dimethine systems in the Dtena unit were 1,3-methine systems, viz. two methines separated by a methylene. Since in each of these cases all six possible conformers can be distinguished from one another based on $^3J_{H,H}$ and $^{2,3}J_{C,H}$ values,[13] the relative configuration and the conformation of the

(11) Luesch, H.; Yoshida, W. Y.; Moore, R. E.; Paul, V. J. *J. Nat. Prod.* **2000**, *63*, 1437−1439.

(12) Luesch, H.; Yoshida, W. Y.; Moore, R. E.; Paul, V. J. *J. Nat. Prod.* **2000**, *63*, 1106−1112.

(13) Matsumori, N.; Kaneno, D.; Murata, M.; Nakamura, H.; Tachibana, K. *J. Org. Chem.* **1999**, *64*, 866−876.

(14) (a) Murata, M.; Matsuoka, S.; Matsumori, N.; Paul, G. K.; Tachibana, K. *J. Am. Chem. Soc.* **1999**, *121*, 870−871. (b) Wu, M.; Okino, T.; Nogle, L. M.; Marquez, B. L.; Williamson, R. T.; Sitachitta, N.; Berman, F. W.; Murray, T. F.; McGough, K.; Jacobs, R.; Colsen, K.; Asano, T.; Yokokawa, F.; Shioiri, T.; Gerwick, W. H. *J. Am. Chem. Soc.* **2000**, *122*, 12041−12042.

(15) Bassarello, C.; Bifulco, G.; Zampella, A.; D'Auria, M. V.; Riccio, R.; Gomez-Paloma, L. *Eur. J. Org. Chem.* **2001**, 39−44.

(16) Uhrín, D.; Barlow, P. N. *J. Magn. Reson.* **1997**, *126*, 248−255.

(17) Uhrín, D.; Batta, G.; Hruby, V. J.; Barlow, P. N.; Kövér, K. E. *J. Magn. Reson.* **1998**, *130*, 155−161.

(18) Williamson, R. T.; Márquez, B. L.; Gerwick, W. H.; Kövér, K. E. *Magn. Reson. Chem.* **2000**, *38*, 265−273.

(19) Wollborn, U.; Leibfritz, D. *J. Magn. Reson.* **1992**, *98*, 142−146.

(20) The diagonal (and geminal) correlation peaks actually appear antiphase, but in the data processing one can choose not to display negative peaks, resulting in an apparent suppression of the diagonal.

(21) A modified HSQMBC pulse sequence incorporating a gradient-BIRD sequence during the INEPT transfer was used (Williamson, R. T., personal communication).

(22) The coupling constants that determine the rotamer for C39−C40 are somewhat outside of the range predicted in ref 13 by displaying more extreme values, but can easily be grouped into "small" or "large".

(23) The rotamers have been denominated as in ref 13.

Table 1. NMR Spectral Data for Apratoxin A (**1**) at 500 MHz (^{1}H) and 125 MHz (^{13}C) in $CDCl_3$

unit	C/H no.	δ_H (J in Hz)	δ_C[a]	^{1}H−^{1}H COSY	HMBC[b]	ROESY
Pro	1		172.6, s		H-2, H-3a, H-3b, H-39	
	2	4.19, t (7.6)	59.8, d	H-3a, H-3b	H-3a	H-3b, H_3-41/42/43
	3a (*pro-R*)	1.88, m	29.3, t	H-2, H-3b	H-2, H-4a	H-3b, H_3-41/42/43
	3b (*pro-S*)	2.23, m		H-2, H-3a		H-2, H-3a
	4a (*pro-S*)	1.90, m	25.6, t	H-4b, H-5a, H-5b	H-2, H-3a, H-3b	H-4b, H-5b
	4b (*pro-R*)	2.05, m		H-4a, H-5a, H-5b	H-5a, H-5b	H-4a, H-5a
	5a (*pro-R*)	3.66, m	47.6, t	H-4a, H-4b	H-3b	H-4b, H-5b, H_3-11
	5b (*pro-S*)	4.23, m		H-4a, H-4b		H-4a, H-5a, H-7
N-Me-Ile	6		170.7, s		H-7	
	7	5.20, d (11.6)	56.6, d	H-8	H_3-11, H_3-12	H-5b, H_3-11, H_3-12
	8	2.24, m	31.8, d	H-7, H_3-11	H-7, H_3-10, H_3-11	H-9b, H_3-11, H_3-12, H-34, OH
	9a	0.96, m	24.7, t	H-9b	H-7, H_3-10, H_3-11	H-9b, H_3-32
	9b	1.31, m		H-9a, H_3-10, H_3-11		H-8, H-9a
	10	0.91, t (7.2)	9.0, q	H-9b	H-9a, H-9b	
	11	0.95, d (6.8)	14.0, q	H-8	H-7, H-9a	H-5a, H-7, H-8, H-34
	12	2.71, s	30.5, q		H-7	H-7, H-8, H-14, H_3-16, H-29, OH
N-Me-Ala	13		170.0, s		H-7, H_3-12, H_3-15	
	14	3.28, br q (6.6)	60.7, d	H_3-15	H_3-15, H_3-16	H_3-12, H_3-15, H_3-16
	15	1.21, d (6.6)	13.9, q	H_3-14		H-14, H_3-16, H-21/25
	16	2.81, s	36.7, q			H_3-12, H-14, H_3-15, H-18, H-21/25
O-Me-Tyr	17		170.4, s		H_3-16, H-19a, H-19b	
	18	5.05, ddd (10.9, 9.4, 4.8)	50.5, d	H-19a, H-19b, NH	H-19a, H-19b, NH	H_3-16, H-19a
	19a	2.86, dd (−12.4, 4.8)	37.2, t	H-18, H-19b	H-18, H-21/25	H-18, H-19b
	19b	3.11, dd (−12.4, 10.9)		H-18, H-19a		H-19a, NH
	20		128.3, s		H-19a, H-19b, H-22/24	
	21/25	7.15, d (8.8)	130.6, d	H-22/24	H-19a, H-19b, H-21/25	H_3-15, H_3-16, H-22/24
	22/24	6.80, d (8.8)	113.9, d	H-21/25	H-21/25, H-22/24	H-21/25
	23		158.7, s		H-21/25, H-22/24, H_3-26	
	26	3.78, s	55.3, q			
	NH	6.04, d (9.4)				H-18b, H_3-32
moCys	27		169.6, s		NH, H-29, H_3-32	
	28		130.5, s		H-30, H_3-32	
	29	6.35, dq (9.7, −1.3)	136.3, d	H-30, H_3-32	H-30, H-31a, H-31b, H_3-32	H_3-12, H-30, H-31a
	30	5.25, ddd (9.7, 8.9, 4.2)	72.5, d	H-29, H-31a, H-31b	H-31a, H-31b	H-29, H-31a, H-31b, H_3-32, OH
	31a (*pro-R*)	3.14, dd (−10.9, 4.2)	37.6, t	H-30	H-29	H-29, H-30, H-31b
	31b (*pro-S*)	3.46, dd (−10.9, 8.9)		H-30		H-30, H-31a
	32	1.96, d (−1.3)	13.3, q	H-29	H-29	H-9a, NH, H-30
Dtena	33		177.4, s		H-30, H-31a, H-31b, H-34, H-35, H_3-44	
	34	2.64, dq (10.0, 7.0)	49.1, d	H-35, H_3-44	H-36b, H_3-44	H-8, H_3-11, H-36b, H_3-44, OH
	35	3.54, dddd (11.4, 10.7, 10.0, 2.9)	71.6, d	H-34, H-36b, OH	H-34, H-36b, H_3-44, OH	H_3-44, H_3-45, OH
	36a (*pro-S*)	1.11, ddd (−13.4, 12.0, 2.9)	38.1, t	H-36b, H-37	H-34, H_3-45, OH	H-36b
	36b (*pro-R*)	1.58, ddd (−13.4, 11.4, 3.9)		H-35, H-36a		H-34, H-36a, H-39, OH
	37	2.16, ddqdd (12.0, 11.8, 6.6, 3.9, 3.4)	24.3, d	H-36a, H-38a, H_3-45	H-36b, H-38a, H-38b, H_3-45	H-38b, H_3-45, OH
	38a (*pro-S*)	1.26, ddd (−13.9, 11.8, 2.3)	37.7, t	H-37, H-38b	H_3-45	H-38b, H-39, H_3-41/42/43
	38b (*pro-R*)	1.79, ddd (−13.9, 12.7, 3.4)		H-38a, H-39		H-37, H-38a, H_3-41/42/43, H_3-45
	39	4.97, dd (12.7, 2.3)	77.4, d	H-38b	H_3-41/42/43	H-36b, H-38a, H_3-41/42/43
	40		34.9, s		H-38b, H_3-41/42/43	
	41/42/43	3 × 0.87, s	3 × 26.0, q		H-39, H_3-41/42/43	H-2, H-3a, H-38a, H-38b, H-39
	44	1.07, d (7.0)	16.6, q	H-34	H-34	H-34, H-35
	45	0.99, d (6.6)	19.8, q	H-37	H-36b, H-38b	H-35, H-37, H-38b
	OH	4.69, d (10.7)		H-35		H-8, H_3-12, H-30, H-34, H-35, H-36b, H-37

[a] Multiplicity deduced from the HSQC spectrum. [b] Protons showing long-range correlation with indicated carbon.

individual units could be determined (Figure 2b−e).[22] Their assemblage, with the aid of the stereospecifically assigned diastereotopic methylene protons, resulted in the elucidation of the relative configuration, including conformation of the Dtena unit in **1**. The proposed conformation was in agreement with all of the NOEs observed within this moiety (Figure 3).

The absolute stereochemistry at C35 was determined as *S* by the modified Mosher method (for $\Delta\delta$ values, see Figure 4).[26] Having established the relative stereochemistry for C33−C39, the absolute configuration of the Dtena unit was consequently 34*S*,35*S*,37*S*,39*S*. This completed the total structure elucidation of **1**.

Molecular Modeling. Molecular modeling provided information about the conformation of apratoxin A (**1**) in solution ($CDCl_3$), a study that did not contradict but rather supported the elucidated stereochemistry. To find 3D structures that were

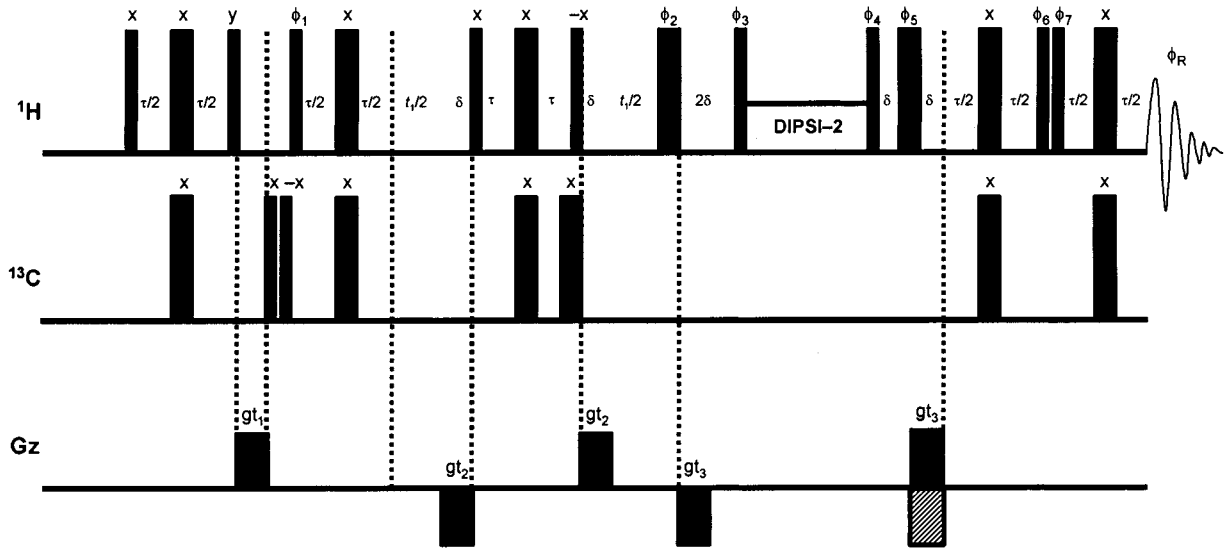

Figure 1. Pulse sequence for the sensitivity- and gradient-enhanced HETLOC[17] with diagonal inversion.[19] Thin and thick bars represent 90° and 180° pulses, respectively; $\tau = (1/2)^1J_{C,H}$, $\phi_1 = 2(y), 2(-y)$, $\phi_2 = 8(x), 8(-x)$, $\phi_3 = 4(x), 4(-x)$, $\phi_4 = \phi_3$, $\phi_5 = \phi_2$, $\phi_6 = 4(y), 4(-y)$, $\phi_7 = 4(-y), 4(y)$, $\phi_R = -x, 2(x), -x$. The pulse preceding the mixing period and final gradient are inverted in adjacent blocks to obtain the hypercomplex quadrature phase in t_1. The following gradient values have been used (in G/cm): $gt_1 = 10$, $gt_2 = 2.5$, $gt_3 = 4$. Rectangular-shaped *z*-gradients were 1 ms in length with a 50 μs recovery delay. The spin-lock period was 60 ms.

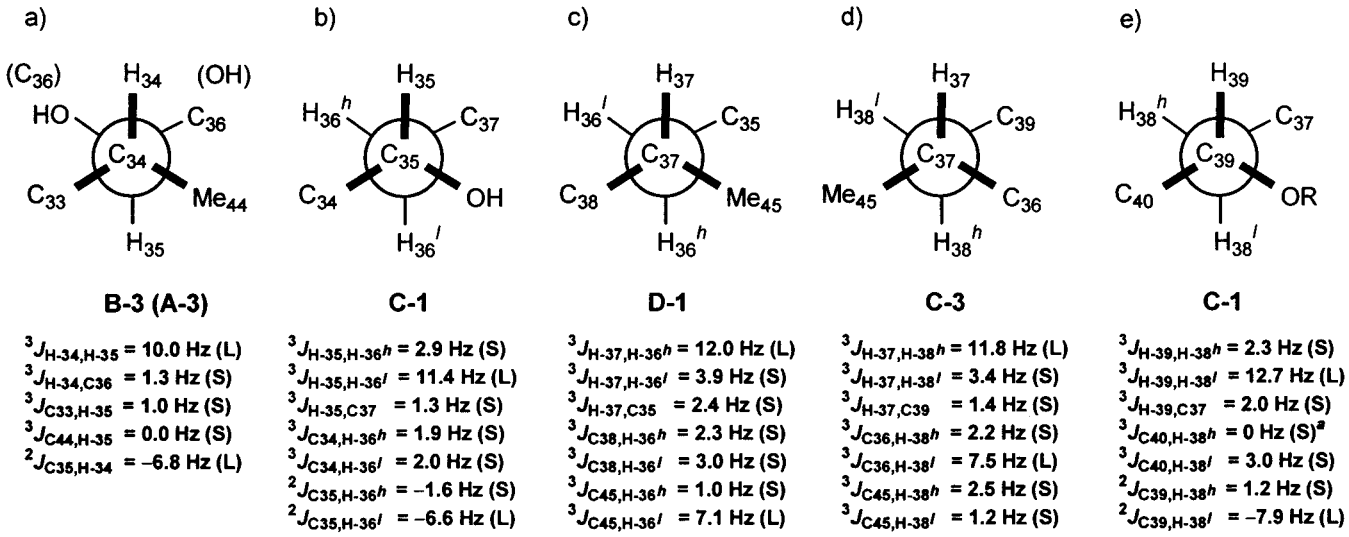

[a] No correlation observed in the HSQMBC experiment as expected for a coupling of 0 Hz.

Figure 2. $^3J_{H,H}$ and $^{2,3}J_{C,H}$ values that led to the assignment of the rotamers with the relative stereochemistry shown for the polyketide portion C33−C45 of apratoxin A (**1**).[23] (S) for "small" and (L) for "large" refer to the magnitude of the coupling constants, resulting in the identification of gauche or anti orientations. For the 1,2-methine system (a), *threo* rotamer A-3 and *erythro* rotamer B-3 could not be distinguished solely based on coupling constants. NOE experiments established the presence of rotamer B-3 (see text). For the 1,3-methine systems (b−e), all rotamers could clearly be identified using the *J*-based configuration analysis.[13,22] H^h and H^l denote the diastereotopic methylene protons observed at higher field and at lower field, respectively.

in agreement with experimental data (NOEs, *J* couplings) and at the same time had low energies in a given force field, we chose a protocol comprised of two steps: First, distance geometry (DG)[27] was used to generate structures that were consistent with the observed NOEs. Second, restrained molecular dynamics (RMD) in combination with restrained energy minimization (REM) served to minimize the high internal energies of these DG structures.[28] Chiral restraints, as well as 60 NOE derived distance restraints obtained from the ROESY spectrum (Table 1) and semiquantitatively classified into strong (<2.5 Å), medium (2.5−3.5 Å), and weak (3.5−5.0 Å),[29] were included in both DG and RMD/REM calculations. ROESY cross-peaks across the macrocycle **1** were very important and indicated that the *N*-Me-Ile residue should be able to come close to the moCys residue and to the 1,2-methine system of the Dtena unit (Table 1); this provided us with a significant conformational restraint.

Simple geometry-optimized structures (without restraints) were used as starting structures for 10 DG calculations. The resulting (and quite diverse) structures did not significantly violate the NOE-derived distance restraints, but expectedly were of high energy arising largely from van der Waals repulsion terms. For the second step of the molecular modeling protocol, in addition to chiral and NOE derived distance restraints, three-bond proton−proton spin-coupling constants between protons in the Dtena unit with typical values for anti orientation ($^3J_{H,H} \geq 10$ Hz) were incorporated, providing five ^3J dihedral

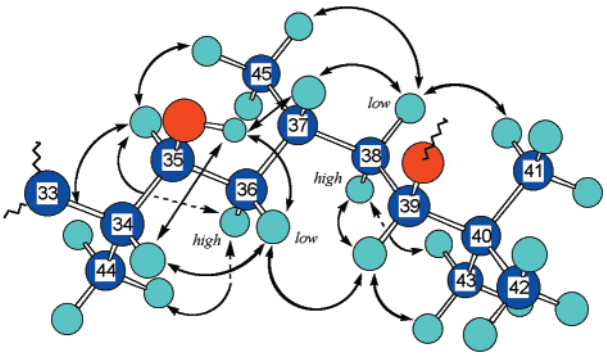

Figure 3. Configuration and conformation of the Dtena moiety in **1** based on $^{3}J_{H,H}$ and $^{2,3}J_{C,H}$ values. NOEs indicated by arrows within this unit support the result of the *J*-based analysis.[13] For the diasterotopic methylene protons, *high* and *low* refer to the highfield and lowfield protons, respectively.

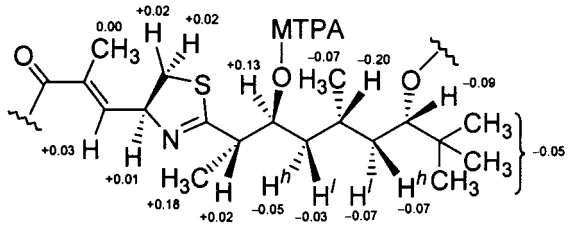

Figure 4. $\Delta\delta$ ($\delta_S - \delta_R$) values for the MTPA esters of **1**.

restraints.[30,31] The 10 DG-optimized structures were subjected to REM to reduce the strain in the molecules. A 10-ps RMD at 500 K was executed to sample the conformational space. Final REM removed the kinetic energy from the systems. Out of the 10 resulting RMD-refined structures, 9 were not only energetically similar, but also belonged to the same conformational family (Figure 5a) and were probably near the global minimum. None of these structures exhibited major violations with respect to the restraints. The 10th structure was of significantly higher energy, violating many distance restraints and even dihedral restraints, and thus was not further considered. The lowest energy conformer found for **1** is shown in Figure 5b. Interestingly, the α,β-unsaturated system in the moCys moiety was not planar in these structures.

The structures after final REM were always considerably lower in energy than after REM that preceded the RMD. This result demonstrates that RMD after DG is superior to only REM after DG, which traps the molecules in local minima. When the dynamics step was run at a lower temperature (300 K) under otherwise identical conditions, essentially the same conformational family resulted. The inclusion of ^{3}J dihedral restraints was deemed necessary, since NOE data did not sufficiently restrict the conformation of the Dtena unit. These additional restraints also lowered the energy and the number of violations of NOE-derived distance restraints in the final structures.[32] Furthermore, the low value chosen for the force constant associated with the NOE-derived distance restraints (1.0 kcal/(mol·Å^2)) was crucial in achieving convergence to a structure that completely satisfied the NMR data.[33] When chiral restraints for the stereocenters in the Dtena unit were switched off, some of the atoms commonly inverted to *R* configuration. However, structures of higher energy and, more importantly, violation of a greater number of distance restraints resulted. The all-*S* configuration appeared indeed to be the best fit for the experimental data.

Biological Activity. Apratoxin A (**1**) exhibits potent cytotoxicity in vitro with IC_{50} values of 0.52 nM against KB and 0.36 nM against LoVo cancer cells.[34] In vivo **1** proved to be toxic to mice and was poorly tolerated at best.[35] A single iv injection of 3.0 mg/kg on day 3 into mice that bore a subcutaneous implanted early stage colon adenocarcinoma gave a T/C of 31%, however, accompanied by drug deaths (LD_{25}) and intolerable weight loss (32% on day 24) of the surviving animals. Sublethal doses, e.g., 1.5 mg/kg/inj on days 3 and 4, produced modest tumor inhibition with a T/C of 51% (inactive by NCI standards) and 21% body weight loss on day 9. Full recovery occurred on day 23, indicating a long (14-day) host recovery time. Against early stage mammary adenocarcinoma 16/C no activity was observed.

The mode of action of **1** is unknown at this time. Apratoxin A (**1**) had no effect on the microfilament network, did not inhibit microtubule polymerization/depolymerization, and did not inhibit topoisomerase I.

Conclusion

Apratoxin A (**1**) is remarkably cytotoxic in vitro as well as in vivo; however, the lack of selectivity limits its potential as an antitumor agent. Structurally, it possesses a novel skeleton and features a *tert*-butyl group in the starter unit for the polyketide synthase that presumably assembles the Dtena moiety. *J*-based configuration analysis was applied successfully

(24) Since the chemical shifts for the H_3-44 (δ 1.07) and the (highfield) H-36a (δ 1.11) were so similar, no direct NOE experiment was possible. Instead, the 1D TOCSY-NOESY method was used.[16] The (lowfield) H-36b (δ 1.58) was selectively excited with a quiet SNEEZE pulse (138.5 ms) in the 1D TOCSY building block, and a second polarization transfer was achieved by selective excitation of the (highfield) H-36a in the 1D NOESY sequence. For the latter excitation, usage of a half-Lorentzian (hL) pulse (72.0 ms) yielded a high sensitivity and ultimately best results. Mixing times were 28 ms for the TOCSY and 500 ms for the NOESY transfer (see Supporting Information).

(25) This result alone suggests already the anti orientation of the substituents. The OH proton gave rise to a sharp doublet (J = 10.7 Hz) in the ^{1}H NMR spectrum and showed other NOEs within the Dtena unit (Table 1), but not to H_3-44 (see Supporting Information).

(26) Ohtani, I.; Kusumi, T.; Kashman, Y.; Kakisawa, H. *J. Am. Chem. Soc.* **1991**, *113*, 4092−4096.

(27) Kuntz, I. D.; Thomason, J. F.; Oshiro, C. M. *Methods Enzymol.* **1989**, *177*, 159−204 and references therein.

(28) (a) Scheek, R. M.; van Gunsteren, W. F.; Kaptein, R. *Methods Enzymol.* **1989**, *177*, 204−218. (b) Kaptein, R.; Boelens, R.; Scheek, R. M.; van Gunsteren, W. F. *Biochemistry* **1988**, *27*, 5389−5395.

(29) Results were found to be independent from the mixing time for $\tau_{mix} \leq$ 500 ms. This is common for small-sized molecules, see, e.g.: Reggelin, M.; Köck, M.; Conde-Frieboes, K.; Mierke, D. *Angew. Chem., Int. Ed. Engl.* **1994**, *33*, 753−755.

(30) A modified Karplus equation, which considers the electronegativity of substituents and their orientation, was used for calculating the torsional angles H−C34−C35−H, H−C35−C36−H^l, H^h−C36−C37−H, and H−C37−C38−H^h: Haasnoot, C. A. G.; de Leeuw, F. A. A. M.; Altona, C. *Tetrahedron* **1980**, *36*, 2783−2792.

(31) The modified Karplus equation by Haasnoot et al.[30] could not account for the large value of $^{3}J_{H-38^l,\,H-39}$ = 12.7 Hz which, however, could be accommodated by a Karplus equation optimized for amino side chains: DeMarco, A.; Llinás, M.; Wüthrich, K. *Biopolymers* **1978**, *17*, 617−636.[22]

(32) The same conclusion was drawn after RMD of a protein: De Vlieg, J.; Boelens, R.; Scheek, R. M.; Kaptein, R.; van Gunsteren, W. F. *Isr. J. Chem.* **1986**, *27*, 181−188.

(33) Other authors had a similar experience, e.g., in modeling a cyclic peptide: Fesik, S. W.; Bolis, G.; Sham, H. L.; Olejniczak, E. T. *Biochemistry* **1987**, *26*, 1851−1859.

(34) The IC_{50} values were determined using the SRB assay: Skehan, P.; Storeng, R.; Scudiero, D.; Monks, A.; McMahon, J.; Vistica, D.; Warren, J. T.; Bokesch, H.; Kenney, S.; Boyd, M. R. *J. Natl. Cancer Inst.* **1990**, *82*, 1107−1112.

(35) In vivo trials were carried out as previously described: Corbett, T.; Valeriote, F.; LoRusso, P.; Polin, L.; Panchapor, C.; Pugh, S.; White, K.; Knight, J.; Demchik, L.; Jones, J.; Jones, L.; Lisow, L. In *Anticancer Drug Development Guide: Preclinical Screening, Clinical Trials, and Approval*; Teicher, B., Ed.; Humana Press Inc.: Totowa, NJ, 1997; pp 75−99.

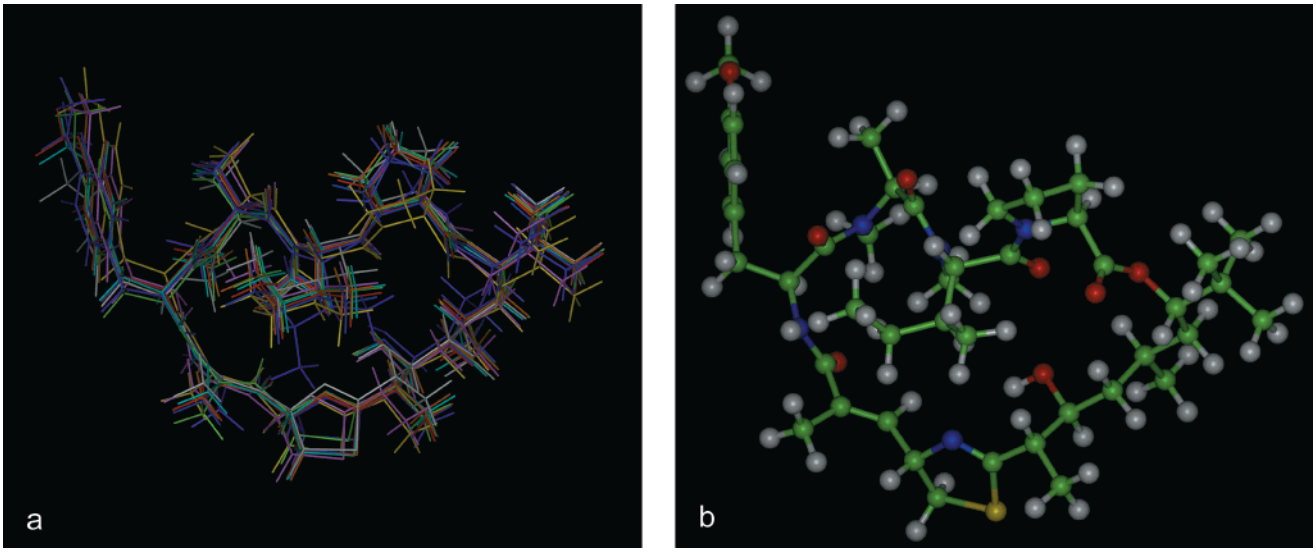

Figure 5. Molecular modeling of apratoxin A (**1**) using distance geometry followed by restrained molecular dynamics: (a) superpositioned stereostructures consistent with NMR data (NOEs, *J* couplings) and (b) lowest energy conformer generated during the simulations.

to elucidate the stereochemistry of this moiety, extending the applicability of the method from acyclic systems to macrocyclic compounds. However, we also share the concern raised earlier that deviations from staggered rotamers might occur,[13] but this is much less likely in macrocyclic systems such as **1** than in smaller ring systems. We feel that *J*-based analysis can predict the relative stereochemistry in nonrigid cyclic systems, especially in conjunction with NOE experiments, more reliably than NOE-based techniques alone or even combined with molecular mechanics. Very similar polyketide portions as in **1** (with unknown stereochemistry) have been found in laingolide,[36] laingolide A,[37] and madangolide[37] isolated from the related *L. bouillonii* from Papua New Guinea, a cyanobacterium that has at least one metabolite, lyngbyapeptin A, in common with our apratoxin A-producing organism.[11,38] Since apratoxin A (**1**) is presumably biosynthesized nonribosomally by modular peptide synthetases and polyketide synthases, valued for their potential use in combinatorial biosynthesis,[39] **1** may be an attractive target for biosynthetic studies on the genetic level.

Acknowledgment. Funding was provided by NCNPDDG grant CA53001 from the National Cancer Institute. The upgrade of the 500 MHz NMR spectrometer used in this research was funded by grants from the CRIF Program of the National Science Foundation (CHE9974921) and the Elsa U. Pardee Foundation. Jason Biggs, Florence Camacho, Frank Camacho, Richard deLoughery, David Ginsburg, Jesse Manglona, Ronald Pangilinan, and Star Shelton assisted with collection and extraction. NIH grant GM 44796 (MBRS program) to V.J.P. provided funding for some of these students. The cyanobacterium was identified by Dr. G. M. L. Patterson, Department of Chemistry, University of Hawaii. General cytotoxicity assays and inhibition of topoisomerase I assays were performed by Dr. M. Lieberman, Department of Chemistry, University of Hawaii. Cytoskeletal assays were carried out in Dr. S. L. Mooberry's laboratory, Cancer Research Center of Hawaii. Mass spectral analyses were conducted by the UCR Mass Spectrometry Facility, Department of Chemistry, University of California at Riverside. We thank Dr. R. T. Williamson, Wyeth-Ayerst Research, Pearl River, NY, and Dr. W. P. Niemczura, Department of Chemistry, University of Hawaii, for helpful discussions regarding the HETLOC and HSQMBC experiments.

Supporting Information Available: Experimental section describing general procedures, methods for measuring $^{2,3}J_{C,H}$ values, biological material, extraction and isolation, physical data for **1**, amino acid analysis, preparation and NMR data for the MTPA esters of **1**, and molecular modeling; ^{1}H NMR, ^{13}C NMR, ^{1}H−^{1}H COSY, HSQC, HMBC, ROESY, and HSQMBC spectra of **1**; a HETLOC spectrum of **1** with and without diagonal suppression; 1D TOCSY-NOESY and 1D NOE spectra used for the assignments of relative configuration of **1**; and ^{1}H NMR spectra of the MTPA esters of **1** (PDF). This material is available free of charge via the Internet at http://pubs.acs.org.

JA010453J

(36) Klein, D.; Braekman, J.-C.; Daloze, D.; Hoffmann, L.; Demoulin, V. *Tetrahedron Lett.* **1996**, *37*, 7519−7520.
(37) Klein, D.; Braekman, J. C.; Daloze, D.; Hoffmann, L.; Castillo, G.; Demoulin, V. *J. Nat. Prod.* **1999**, *62*, 934−936.
(38) Klein, D.; Braekman, J.-C.; Daloze, D.; Hoffmann, L.; Castillo, G.; Demoulin, V. *Tetrahedron Lett.* **1999**, *40*, 695−696.
(39) (a) Khosla, C. *Chem. Rev.* **1997**, *97*, 2577−2590. (b) Marahiel, M. A.; Stachelhaus, T.; Mootz, H. D. *Chem. Rev.* **1997**, *97*, 2651−2673.